Available online at www.sciencedirect.com
ScienceDirect
International Journal of Heat and Mass Transfer 50 (2007) 949–959
International Journal of HEAT and MASS TRANSFER
www.elsevier.com/locate/ijhmt

Unsteady mixed convection flow over a vertical cone due to impulsive motion

Param Jeet Singh, S. Roy *

Department of Mathematics, Indian Institute of Technology Madras, Chennai 600 036, India

Received 15 March 2006
Available online 23 October 2006

Abstract

The development of unsteady mixed convection flow of an incompressible laminar viscous fluid over a vertical cone has been investigated when the fluid in the external stream is set into motion impulsively, and at the same time the surface temperature is suddenly changed from its ambient temperature. The problem is formulated in such a way that at $t = 0$, it reduces to Rayleigh type of equation and as $t \to \infty$, it tends to Falkner–Skan type of equation. The scale of time has been selected such that the traditional infinite region of integration become finite which significantly reduce the computational time. The coupled non-linear partial differential equations governing the unsteady mixed convection flow have been solved numerically by using an implicit finite-difference scheme in combination with the quasi-linearization technique. There is a smooth transition from the initial steady state to the final steady state. The velocity, temperature, and concentration profiles and their gradients at the surface for various values of the governing parameters are reported in the present study.

1. Introduction

Free convection is caused by the temperature difference of the fluid at different locations and forced convection is the flow of heat due to the cause of some external applied forces. The combination of both of these phenomena is called the mixed convection. The phenomenon of mixed convection occurs in many technical and industrial problems like electronic devices cooled by fans, nuclear reactor cooled during emergency shutdown, heat exchanger placed in a low velocity environment, solar central receiver to wind current etc. The system to be studied in the present investigation, shown schematically in Fig. 1, is a vertical cone in a viscous fluid when the axis of the cone is inline with the flow. If the cone surface and free stream fluid temperature differ, not only energy will be transferred to the flow but also density difference will exist. In a gravitational field these density differences result in an additional force, buoyancy force, beside viscous force due to the viscous action. In many practical circumstances of moderate flow velocities and large wall-fluid temperature differences, the magnitude of buoyancy force and viscous force are of comparable order and convective heat transfer process is considered as mixed convection. Cone shaped bodies are often encountered in many engineering application and many heat transfer problems of mixed convection boundary layer flow over a stationary cone, which occur in stationary heat exchangers, are extensively used by chemical and auto-mobile industries. Moreover, convective heat transfer on a stationary cone has several important applications such as design of canisters for nuclear waste disposal, nuclear reactor cooling system, geothermal reservoirs etc. Laminar boundary layer flows exhibiting similarity have long played an important role in exposing the influence of physical, dynamical and thermal parameters without introducing the complications

* Corresponding author. Tel.: +91 44 2257 8492; fax: +91 44 2257 4602.
E-mail addresses: paramjeet@iitm.ac.in (P.J. Singh), sjroy@iitm.ac.in (S. Roy).
URL: http://mat.iitm.ac.in/s~jroy (S. Roy).

0017-9310/$ - see front matter © 2006 Elsevier Ltd. All rights reserved.
doi:10.1016/j.ijheatmasstransfer.2006.08.011

Nomenclature

C_f	skin friction coefficient
C	species concentration
f	dimensionless stream function
F	dimensionless velocity along the x-direction
g	acceleration due to gravity
Gr_L, Gr_L^*	Grashof numbers
N	ratio of the buoyancy parameters
Nu	Nusselt numbers
Pr	Prandtl number
Re_L	Reynold number
Sc	Schmidt number
Sh	Sherwood number
t	time
T	temperature
T_w	temperature at the wall
u, v	tangential and azimuthal velocity components

Greek symbols

α	semi vertical angle of the cone
β	volumetric coefficient of thermal expansion
β^*	volumetric coefficient of expansion for concentration
η	similarity variable
θ	dimensionless temperature
λ, λ^*	buoyancy parameters
μ	dynamic viscosity
ν	kinematic viscosity of the fluid
ξ	transformed coordinate
ρ	density of the fluid
ϕ	dimensionless concentration
ψ	dimensional stream function

Subscripts

i, ∞, w, e	denote the initial conditions, conditions in the free stream, at the wall and at the edge of the boundary layer, respectively
ξ, η	denote the partial derivatives w.r.t to these variables, respectively
x, y	denote the partial derivatives w.r.t to these variables, respectively

of non-similar solutions and in providing bases for approximate methods of calculating more complex non-similar cases. In case when the conditions for similarity are satisfied, the complex set of partial differential equations governing the flow transformed to a system of ordinary differential equations which evidently constitute a considerable mathematical simplification of the problem. A solution is called self-similar if a system of partial differential equations can be reduced to a system of ordinary differential equations. If the similarity transformation are only able to reduce the number of independent variables, then the transformed equations are known as semi-similar and the corresponding solutions are the semi-similar solutions [1].

Early work of Hering and Grosh [2] presents a number of similarity solutions for cones, with prescribed wall temperature being a power function of the distance from the apex along the generator. Further investigation of this problem for low Pr number were made by Hering [3], and Sparrow and Guinle [4], while for large Pr number were made by Roy [5]. Later, Hasen and Majumdar [6] have investigated the steady double diffusive mixed convection flow along a vertical cone under the combined buoyancy effect of thermal and species diffusion. The local similarity method has been employed to solve the transformed non-dimensional equations. Subsequently, Kumari et al. [7] have studied the problem of steady mixed convection flow along an isothermal vertical cone and the transformed non-dimensional equations of the non-similar boundary layers are solved by efficient finite-difference method. Recently, Roy and Anil kumar [1] have obtained a semi-similar solution of an unsteady mixed convection flow over a rotating cone in a rotating viscous fluid when the free stream angular velocity and angular velocity of the cone vary arbitrarily with time. In many practical problems, the flow could be unsteady due to the angular velocity of the spinning body which varies with time or due to the impulsive change in the velocity of the body or due to the free stream velocity which varies with time. The flow and heat transfer development of boundary layer in an impulsively rotating and translating axi-symmetric body was considered by Ece [8]. To obtain the solution for small values of time, Kumari [9] studied the temporal development of flow and heat transfer over a wedge with a magnetic field caused by the impulsive motion of the free stream velocity and sudden change in the wall temperature. The governing boundary layer equations were solved numerically by implicit finite-difference scheme and solutions are valid for all times. Recently, Seshadri et al. [10] have studied the unsteady mixed convection in a stagnation flow adjacent to a heated vertical surface where the unsteadiness is caused by the impulsive motion of the free stream velocity as well as sudden increase in the wall temperature. The parabolic partial differential equation governing the boundary layer flow have been solved by using an implicit finite-difference scheme starting from the initial steady state to final steady state. William and Rhyne [11] describe the boundary layer development on a wedge impulsively set into motion and the method to obtain the transformation is explained in their study.

The aim of the present study is to investigate the simultaneous effects of impulse on an unsteady mixed convection flow over a vertical cone including the effect of thermal and

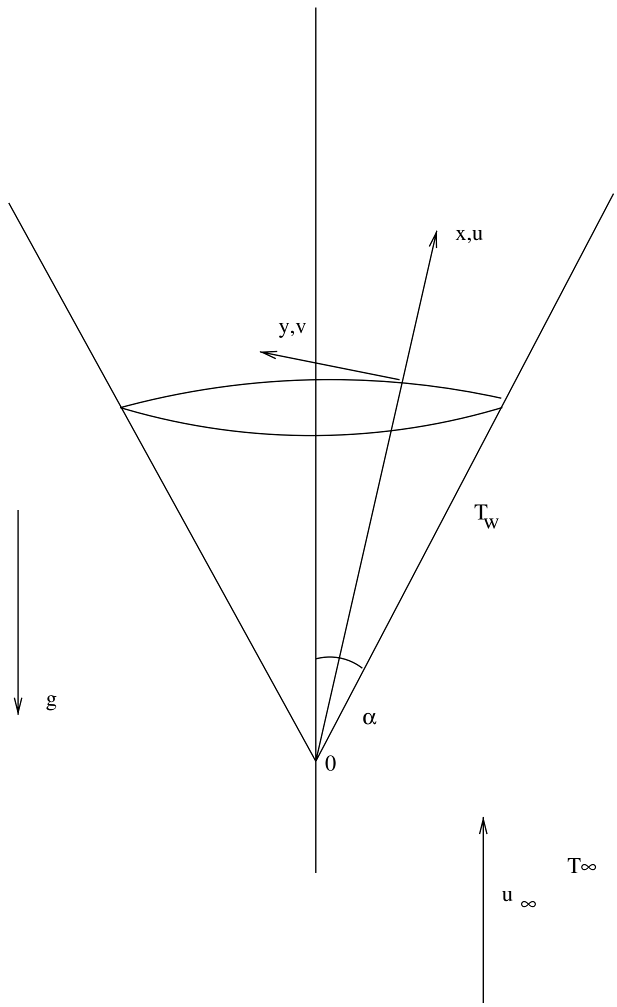

Fig. 1. Physical model and coordinate system.

mass diffusions. The unsteadiness is caused by the impulsive motion of the vertical cone. The problem is formulated in such a way that at time $t = 0$, it is governed by Rayleigh type of equation and as $t \to \infty$, it is governed by Falkner–Skan type of equation. The semi-similar solution of coupled non-linear partial differential equations governing the mixed convection flow has been obtained numerically using the quasi-linearization technique in combination with an implicit finite-difference scheme. The results have been compared with Seshadri et al. [10] and William and Rhyne [11], and found in an excellent agreement.

2. Analysis

Consider an unsteady mixed convection flow over a vertical cone impulsively set into motion. The unsteadiness caused due to the impulsive motion of the cone. The coordinate system and the physical model are shown in Fig. 1. The buoyancy forces arise by both the variation in the temperature and concentration of fluid and the flow is taken to be axi-symmetric. All the properties of the fluid are constant except the density variations causing the buoyancy force term in the momentum equation. Both the temperature and concentration at the wall vary as a function of x. The Boussinesq approximation is invoked for the fluid properties to relate the density change to temperature and concentration changes and to couple in this way the temperature and concentration field to the flow field. Under the above assumptions, and imposing the Mangler's transformation to [12] reduce the axi-symmetric problem into a two-dimensional problem, the governing boundary layer momentum, energy and concentration equations are

$$u_x + v_y = 0, \tag{1}$$

$$u_t + uu_x + vu_y = u_e(u_e)_x + \nu u_{yy} + [g\beta(T - T_\infty) + g\beta^\star(C - C_\infty)]\cos\alpha, \tag{2}$$

$$T_t + uT_x + vT_y = Pr^{-1}\nu T_{yy}, \tag{3}$$

$$C_t + uC_x + vC_y = Sc^{-1}\nu C_{yy}. \tag{4}$$

The initial conditions are

$$u(x,y,0) = u_i(x,y), \quad v(x,y,0) = v_i(x,y),$$
$$T(x,y,0) = T_i(x,y), \quad C(x,y,0) = C_i(x,y), \tag{5}$$

and the boundary conditions are given by

$$u(x,0,t) = v(x,0,t) = 0, \quad T(x,0,t) = T_w,$$
$$C(x,0,t) = C_w, \quad u(x,\infty,t) = u_e(x) = u_\infty x^{m/3},$$
$$v(x,\infty,t) = 0, \quad T(x,\infty,t) = T_\infty, \quad C(x,\infty,t) = C_\infty. \tag{6}$$

Here α is the semi vertical angle of the cone; ν is the kinematic viscosity of the fluid; ρ is the density; g is the acceleration due to gravity; T is the temperature; C is the species concentration; β is volumetric coefficient of thermal expansion; β^* is the volumetric coefficient of expansion for concentration; t is the time; Pr is the Prandtl number; Sc is the Schmidt number; subscripts x and y denote the partial derivatives with respect to the corresponding variables and the subscripts i, ∞, w and e denote the initial conditions, the conditions in the free stream, the conditions at the surface and the conditions at the edge of the boundary layer, respectively; C_∞ and T_∞ are constants.

Applying the following transformations:

$$\eta = \left(\frac{u_e}{x\xi\nu}\right)^{\frac{1}{2}} y, \quad \xi = 1 - \exp(-t^*), \quad t^* = \frac{u_e t}{x} = u_\infty(x)^{\frac{m-3}{3}} t,$$

$$\psi(x,y,t) = (xu_e\nu\xi)^{1/2} f(\xi,\eta), \quad \frac{\partial\psi}{\partial y} = u, \quad \frac{\partial\psi}{\partial x} = -v,$$

$$u = u_e f_\eta(\xi,\eta) = u_e F(\xi,\eta), \quad f_\eta(\xi,\eta) = F(\xi,\eta),$$

$$v = -\left[\frac{1}{2}\left(\frac{\nu u_e \xi}{x}\right)^{\frac{1}{2}} f + \frac{1}{2}\left(\frac{\nu u_e x}{\xi}\right)^{\frac{1}{2}} e^{-t^*} u_\infty \left(\frac{m-3}{3}\right) x^{\frac{m-6}{3}} t f + \frac{1}{2}\left(\frac{\nu x \xi}{u_e}\right)^{\frac{1}{2}} u_\infty \left(\frac{m}{3}\right) x^{\frac{m-3}{3}} f + (x\xi \nu u_e)^{\frac{1}{2}}\left[e^{-t^*} u_\infty \left(\frac{m-3}{3}\right) x^{\frac{m-6}{3}} t \frac{\partial f}{\partial \xi} + f_\eta\left[-\frac{y}{2x}\left(\frac{u_e}{\nu \xi x}\right)^{\frac{1}{2}} - \frac{y}{2\xi}\left(\frac{u_e}{\nu x \xi}\right)^{\frac{1}{2}} e^{-t^*} u_\infty \left(\frac{m-3}{3}\right) x^{\frac{m-6}{3}} t + \frac{y}{2}\left(\frac{1}{x\nu \xi u_e}\right)^{\frac{1}{2}} u_\infty \left(\frac{m}{3}\right) x^{\frac{m-3}{3}}\right]\right]\right],$$

$$\theta(\xi,\eta) = \frac{T - T_\infty}{T_w - T_\infty}, \quad T_w = T_\infty + (T_{w0} - T_\infty)L(x)^{(2m-3)/3},$$

$$\phi(\xi,\eta) = \frac{C - C_\infty}{C_w - C_\infty}, \quad C_w = C_\infty + (C_{w0} - C_\infty)L(x)^{(2m-3)/3}, \tag{7}$$

to Eqs. (1)–(4), we find that Eq. (1) is identically satisfied, and Eqs. (2)–(4) reduce to

$$F_{\eta\eta} + fF_\eta\left[\xi\left(\frac{m+3}{6}\right) - (1-\xi)\left(\frac{m-3}{6}\right)\log(1-\xi)\right] + \frac{\eta}{2}(1-\xi)F_\eta - \xi(1-\xi)\frac{\partial F}{\partial \xi} + \frac{m}{3}\xi(1-F^2) + \lambda\xi(\theta + N\phi) = \frac{\xi}{3}(m-3)(1-\xi)\log(1-\xi)\left[F_\eta \frac{\partial f}{\partial \xi} - F\frac{\partial F}{\partial \xi}\right], \tag{8}$$

$$\theta_{\eta\eta} + Prf\theta_\eta\left[\left(\frac{m+3}{6}\right)\xi - \left(\frac{m-3}{6}\right)(1-\xi)\log(1-\xi)\right] + Pr\frac{\eta}{2}(1-\xi)\theta_\eta - Pr\left(\frac{2m-3}{3}\right)\xi F\theta = Pr(1-\xi)\log(1-\xi)\xi\left(\frac{m-3}{3}\right)\left[\theta_\eta\frac{\partial f}{\partial \xi} - F\frac{\partial \theta}{\partial \xi}\right] + Pr(1-\xi)\xi\frac{\partial \theta}{\partial \xi}, \tag{9}$$

$$\phi_{\eta\eta} + Scf\phi\eta\left[\left(\frac{m+3}{6}\right)\xi - \left(\frac{m-3}{6}\right)(1-\xi)\log(1-\xi)\right] + Sc\frac{\eta}{2}(1-\xi)\phi_\eta - Sc\left(\frac{2m-3}{3}\right)\xi F\phi = Sc(1-\xi)\log(1-\xi)\xi\left(\frac{m-3}{3}\right)\left[\phi_\eta\frac{\partial f}{\partial \xi} - F\frac{\partial \phi}{\partial \xi}\right] + Sc(1-\xi)\xi\frac{\partial \phi}{\partial \xi}. \tag{10}$$

The boundary conditions reduce to

$$F(\xi,0) = 0, \quad \theta(\xi,0) = \phi(\xi,0) = 1,$$
$$F(\xi,\infty) = 1, \quad \theta(\xi,\infty) = \phi(\xi,\infty) = 0, \tag{11}$$

where

$$Gr_L = \frac{g\beta(T_{w0} - T_\infty)L^3\cos\alpha}{\nu^2},$$
$$Gr_L^* = \frac{g\beta^*(C_{w0} - C_\infty)L^3\cos\alpha}{\nu^2}, \quad Re = \frac{u_\infty L}{\nu}, \quad \lambda = \frac{Gr_L}{Re_L^2},$$
$$\lambda^* = \frac{Gr_L^*}{Re_L^2}, \quad N = \frac{\lambda^*}{\lambda},$$

and

$$f(\xi,\eta) = \int_0^\eta F(\xi,\eta)\,d\eta.$$

Here ξ and η are the transformed coordinates; f is the dimensionless stream function; F is the dimensionless velocity along the x-direction; θ and ϕ are the temperature and concentration; Re_L is the Reynolds number; Gr_L and Gr_L^* are the Grashof numbers; λ and λ^* are the buoyancy parameters; N is the ratio of the buoyancy parameters.

Eqs. (8)–(10) for $\xi = 0$ and $\xi = 1$ reduce to the ordinary differential equations. For $\xi = 0$, they are given by

$$F_{\eta\eta} + \frac{\eta}{2}F_\eta = 0, \tag{12}$$

$$\theta_{\eta\eta} + Pr\frac{\eta}{2}\theta_\eta = 0, \tag{13}$$

$$\phi_{\eta\eta} + Sc\frac{\eta}{2}\phi_\eta = 0. \tag{14}$$

Similarly, for $\xi = 1$ Eqs. (8)–(10) can be expressed as

$$F_{\eta\eta} + \frac{m+3}{6}fF_\eta + \frac{m}{3}(1-F^2) + \lambda(\theta + N\phi) = 0, \tag{15}$$

$$\theta_{\eta\eta} + Pr\frac{m+3}{6}f\theta_\eta - Pr\frac{2m-3}{3}F\theta = 0, \tag{16}$$

$$\phi_{\eta\eta} + Sc\frac{m+3}{6}f\phi_\eta - Sc\frac{2m-3}{3}F\phi = 0. \tag{17}$$

The boundary conditions for Eqs. (12)–(14) or Eqs. (15)–(17) are

$$F(0) = 0, \quad \theta(0) = \phi(0) = 1, \quad F(\infty) = 1,$$
$$\theta(\infty) = \phi(\infty) = 0. \tag{18}$$

The local skin friction coefficient is given by

$$C_f = \frac{2\left[\mu\frac{\partial u}{\partial y}\right]_{y=0}}{(u_e)^2\rho} = 2\xi^{-1/2}Re_L^{-1/2}F_\eta(\xi,0).$$

Thus

$$Re_L^{1/2}C_f = 2\xi^{-1/2}F_\eta(\xi,0).$$

The local Nusselt and Sherwood numbers are expressed as

$$Re_L^{-1/2}Nu = -\xi^{-1/2}\theta_\eta(\xi,0),$$
$$Re_L^{-1/2}Sh = -\xi^{-1/2}\phi_\eta(\xi,0),$$

where

$$Nu = -\frac{\left[x\frac{\partial T}{\partial y}\right]_{y=0}}{T_w - T_\infty} \quad \text{and} \quad Sh = -\frac{\left[x\frac{\partial C}{\partial y}\right]_{y=0}}{C_w - C_\infty}$$

3. Analytic solution

The solution of the linear equations (12)–(14) under conditions (18) can be expressed as

$$f(\eta) = \eta\,\mathrm{erf}(\eta/2) - (\pi)^{-\frac{1}{2}}[1-\exp(-\eta^2/4)], \tag{19}$$

$$F = (\pi)^{-\frac{1}{2}}\mathrm{erf}(\eta/2), \tag{20}$$

$$\theta(\eta) = 1 - \mathrm{erf}\left(Pr^{1/2}\frac{\eta}{2}\right) = \mathrm{erfc}\left(Pr^{1/2}\frac{\eta}{2}\right), \tag{21}$$

$$\phi(\eta) = 1 - \mathrm{erf}\left(Sc^{1/2}\frac{\eta}{2}\right) = \mathrm{erfc}\left(Sc^{1/2}\frac{\eta}{2}\right), \tag{22}$$

$$f_{\eta\eta}(0) = (\pi)^{-1/2}, \quad \theta_\eta(0) = -\left(\frac{Pr}{\pi}\right)^{1/2}, \quad \phi_\eta(0) = -\left(\frac{Sc}{\pi}\right)^{1/2}. \tag{23}$$

It may be noted that Eqs. (12)–(14) for $\xi = 0$ and (15)–(17) for $\xi = 1$ under boundary conditions (18) are identical to Seshadri et al. [11].

4. Method of solution

The non-linear coupled partial differential equations (8)–(10) under the boundary conditions (11) and initial conditions (19)–(22) has been solved numerically using an implicit finite-difference scheme in combination with the quasi-linearization technique. An iterative sequence of linear equations are carefully constructed to approximate the non-linear equations (8)–(10) for achieving quadratic convergence. Applying quasi-linearization technique, the non-linear coupled partial differential equations (8)–(10) are replaced by the following sequence of linear partial differential equations:

$$F_{\eta\eta}^{i+1} + X_1^i F_\eta^{i+1} + X_2^i F^{i+1} + X_3^i F_\xi^{i+1} + X_4^i \theta^{i+1} + X_5^i \phi^{i+1} = X_6^i, \tag{24}$$

$$\theta_{\eta\eta}^{i+1} + Y_1^i \theta_\eta^{i+1} + Y_2^i \theta^{i+1} + Y_3^i \theta_\xi^{i+1} + Y_4^i F^{i+1} + Y_5^i \phi^{i+1} = Y_6^i, \tag{25}$$

$$\phi_{\eta\eta}^{i+1} + Z_1^i \phi_\eta^{i+1} + Z_2^i \phi^{i+1} + Z_3^i \phi_\xi^{i+1} + Z_4^i F^{i+1} + Z_5^i \theta^{i+1} = Z_6^i. \tag{26}$$

The coefficient function with iterative index i are known and the functions with iterative index $i+1$ are to be determined. The boundary conditions are given by

$$F^{i+1} = 0, \quad \theta^{i+1} = \phi^{i+1} = 1 \quad \text{at } \eta = 0,$$
$$F^{i+1} = 1 \quad \theta^{i+1} = \phi^{i+1} = 0, \quad \text{at } \eta = \eta_\infty, \tag{27}$$

where η_∞ is the edge of the boundary layer. The coefficients in Eqs. (24)–(26) are given by

$$X_1 = f\left[\frac{m+3}{6}\xi - \frac{m-3}{6}(1-\xi)\log(1-\xi)\right] + \frac{\eta}{2}(1-\xi) - \frac{m-3}{3}\xi(1-\xi)\log(1-\xi)\frac{\partial f}{\partial \xi},$$

$$X_2 = -\frac{2m}{3}\xi F + \frac{m-3}{3}\xi(1-\xi)\log(1-\xi)\frac{\partial F}{\partial \xi},$$

$$X_3 = -\xi(1-\xi) + \frac{m-3}{3}\xi(1-\xi)\log(1-\xi)F,$$

$$X_4 = \lambda\xi,$$

$$X_5 = \lambda\xi N,$$

$$X_6 = -\frac{m}{3}\xi(1+F^2) + \frac{m-3}{3}\xi(1-\xi)\log(1-\xi)F\frac{\partial F}{\partial \xi},$$

$$Y_1 = Pr\left[f\left[\frac{m+3}{6}\xi - \left(\frac{m-3}{6}\right)(1-\xi)\log(1-\xi)\right] + \frac{\eta}{2}(1-\xi) - \frac{m-3}{3}\xi(1-\xi)\log(1-\xi)\frac{\partial f}{\partial \xi}\right],$$

$$Y_2 = -\frac{2m-3}{3}\xi F Pr,$$

$$Y_3 = Pr\left[\frac{m-3}{3}\xi(1-\xi)\log(1-\xi)F - \xi(1-\xi)\right],$$

$$Y_4 = Pr\left[-\frac{2m-3}{3}\xi\theta + \frac{m-3}{3}\xi(1-\xi)\log(1-\xi)\frac{\partial \theta}{\partial \xi}\right],$$

$$Y_5 = 0,$$

$$Y_6 = Pr\left[-\frac{2m-3}{3}\xi F\theta + \frac{m-3}{3}\xi(1-\xi)\log(1-\xi)F\frac{\partial \theta}{\partial \xi}\right],$$

$$Z_1 = Sc\left[f\left[\left(\frac{m+3}{6}\right)\xi - \left(\frac{m-3}{6}\right)(1-\xi)\log(1-\xi)\right] + \frac{\eta}{2}(1-\xi) - \frac{m-3}{3}\xi(1-\xi)\log(1-\xi)\frac{\partial f}{\partial \xi}\right],$$

$$Z_2 = -\frac{2m-3}{3}\xi F Sc,$$

$$Z_3 = Sc\left[\frac{m-3}{3}\xi(1-\xi)\log(1-\xi)F - \xi(1-\xi)\right],$$

$$Z_4 = Sc\left[-\frac{2m-3}{3}\xi\phi + \frac{m-3}{3}\xi(1-\xi)\log(1-\xi)\frac{\partial \phi}{\partial \xi}\right],$$

$$Z_5 = 0,$$

$$Z_6 = Sc\left[-\frac{2m-3}{3}\xi F\phi + \frac{m-3}{3}\xi(1-\xi)\log(1-\xi)F\frac{\partial \phi}{\partial \xi}\right].$$

Since the method is described for ordinary differential equations by Inouye and Tate [13] and also explained for partial differential equations in a recent article by Roy and Saikrishnan [14], its detailed description is not provided for the sake of brevity. At each iteration step, the sequence of linear partial differential equations (24)–(26) were expressed in difference form using central difference scheme in the η-direction and backward difference scheme in ξ-direction. In each iteration step, these equations were then reduced to a system of linear algebraic equations with a block tri-diagonal matrix, which is solved by Varga's algorithm [15]. To ensure the convergence of the numerical solution to the exact solution, the step sizes $\Delta\eta$ and $\Delta\xi$ have been optimized and the results presented here are independent of the step sizes at least up to the fourth decimal place. The step sizes of $\Delta\eta$ and $\Delta\xi$ have been taken as 0.01 and 0.01, respectively. A convergence criterion based on the relative difference between the current and previous value is employed. When the difference reaches 10^{-4}, the solution is assumed to have converged and the iterative process is terminated.

5. Result and discussion

Computations have been carried out for the various values of Pr $(0.7 \leqslant Pr \leqslant 10.0)$, Sc $(0.22 \leqslant Sc \leqslant 2.57)$, λ $(-10.0 \leqslant \lambda \leqslant 10.0)$ and N $(-1.0 \leqslant N \leqslant 1.0)$. In all numerical computations, the value of m is taken as 4 and the edge of the boundary layer has been taken between 3 and 5 depending on the values of the parameters. In order to verify the correctness of our method, we have compared our results for the surface shear stress parameter($F_\eta(\xi,0)$) with Seshadri et al. [10] and William and Rhyne [11] and surface heat transfer parameter $(-\theta_\eta(\xi,0))$ with the Seshadri et al. [10] for $\lambda = 0$, $N = 0$, $Pr = 0.7$ and $Sc = 0.22$. The skin friction and heat transfer coefficients $(2^{-1}C_f Re_L^{1/2}, 2^{-1}NuRe_L^{-1/2})$ are again compared with Seshadri et al. [10]. The results are matched in excellent agreement and only some of the comparisons are shown in Figs. 2 and 3 to brief the manuscript.

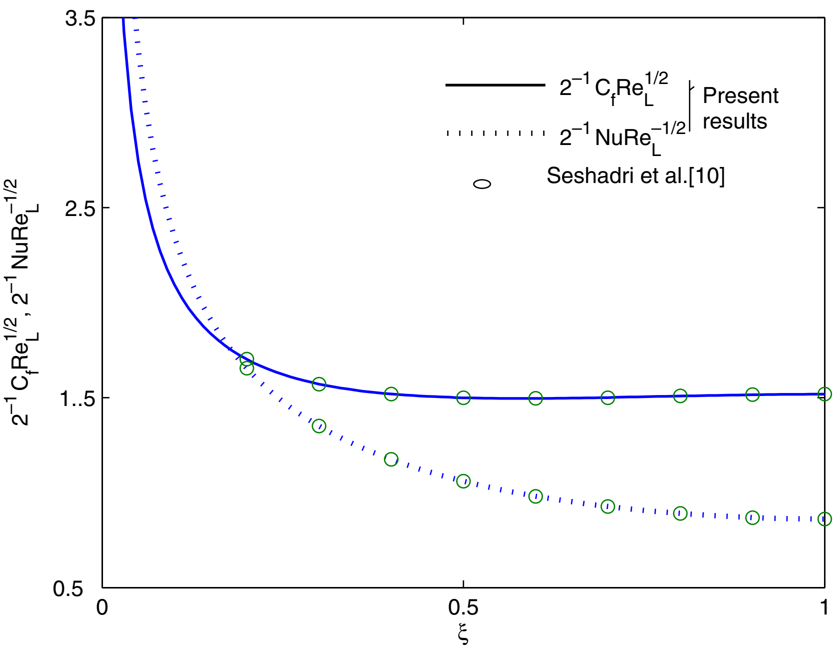

Fig. 2. Comparison of skin friction and heat transfer coefficients for $\lambda = 1$, $N = 0$ with the results of Seshadri et al. [10].

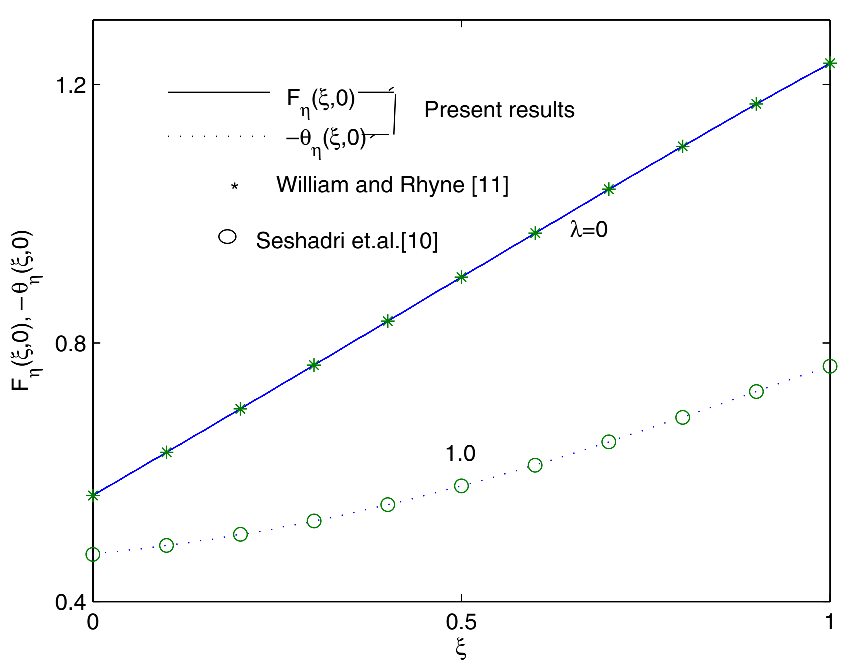

Fig. 3. Comparison of the shear stress and heat transfer parameters with the results of Seshadri et al. [10] and William and Rhyne [11].

The effects of buoyancy parameter λ and Prandtl number (Pr) on velocity and temperature profiles (F, θ) are displayed in Figs. 4 and 5. The variations in the concentration profiles due to the effects of λ and Pr are within 5% and the profiles are not displayed here for the sake of brevity. In buoyancy aiding flow ($\lambda > 0$), the buoyancy force shows the significant overshoot in the velocity profiles near the wall for lower Prandtl number fluid but for higher Prandtl number fluid the velocity overshoot is not much significant as can be observed in Fig. 4. The magnitude of the overshoot increases with the buoyancy parameter λ ($\lambda > 0$) but decreases as the Prandtl number increases. The reason is that the buoyancy force (λ) effect is more in low Prandtl number fluid (air, $Pr = 0.7$) due to the low viscosity of the fluid, which increases the velocity within the boundary layer as the assisting buoyancy force acts like a favorable

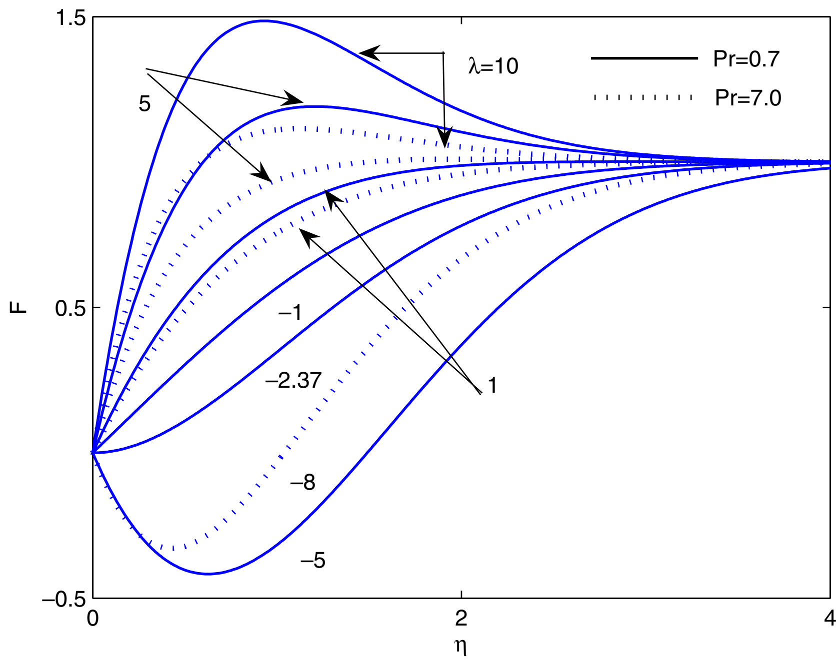

Fig. 4. Effects of Pr and λ on the velocity profile when $N = 0.5$ and $Sc = 0.94$ at $\xi = 0.5$.

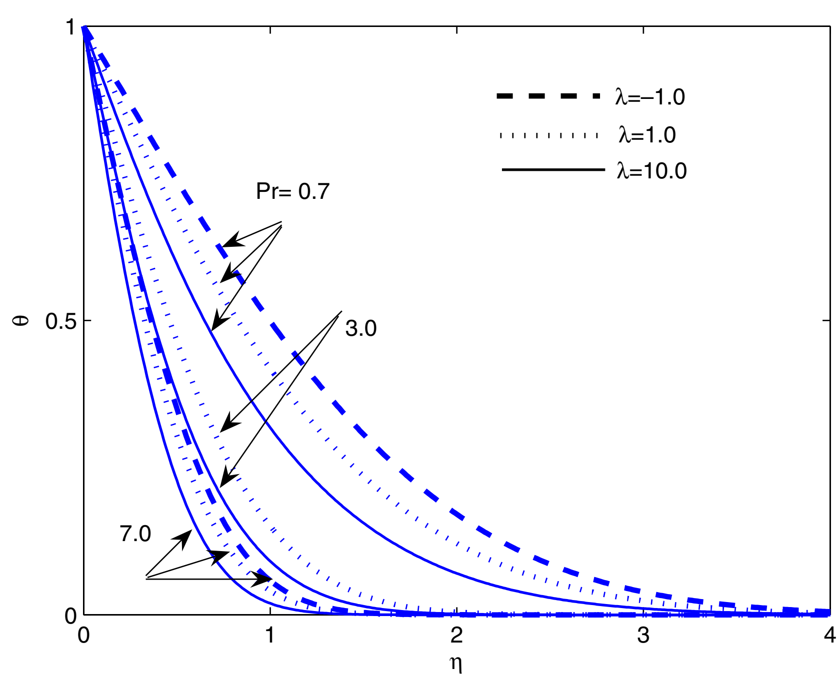

Fig. 5. Effects of Pr and λ on the temperature profile when $N = 0.5$ and $Sc = 0.94$ at $\xi = 0.5$.

pressure gradient. Hence the velocity overshoot occurs and for higher Prandtl number fluids the overshoot is not much significant because higher Prandtl number (water, $Pr = 7.0$), implies more viscous fluid which makes it less sensitive to the buoyancy parameter (λ). It is interesting to notice in Fig. 4 that at $\xi = 0.5$, for buoyancy opposing flow i.e. for negative values of buoyancy parameter λ ($\lambda < 0$), the reverse flow starts at $\lambda \simeq -2.37$ for $Pr = 0.7$ (air) and at $\lambda \simeq -3.43$ for $Pr = 7.0$ (water). The buoyancy opposing force reduces the velocity near the wall subsequently as the buoyancy parameter λ decreases further and the fluid flows backward near the wall in a small region as can be seen in Fig. 4 for $\lambda = -5$ when $Pr = 0.7$ and for $\lambda = -8$ when $Pr = 7.0$. The effect of λ is comparatively less in temperature profile as shown in Fig. 5. Moreover, Fig. 5 shows that the effect of Prandtl number (Pr) results into the thinner thermal boundary layer as the higher Prandtl number (water, $Pr = 7.0$) has a lower thermal conductivity.

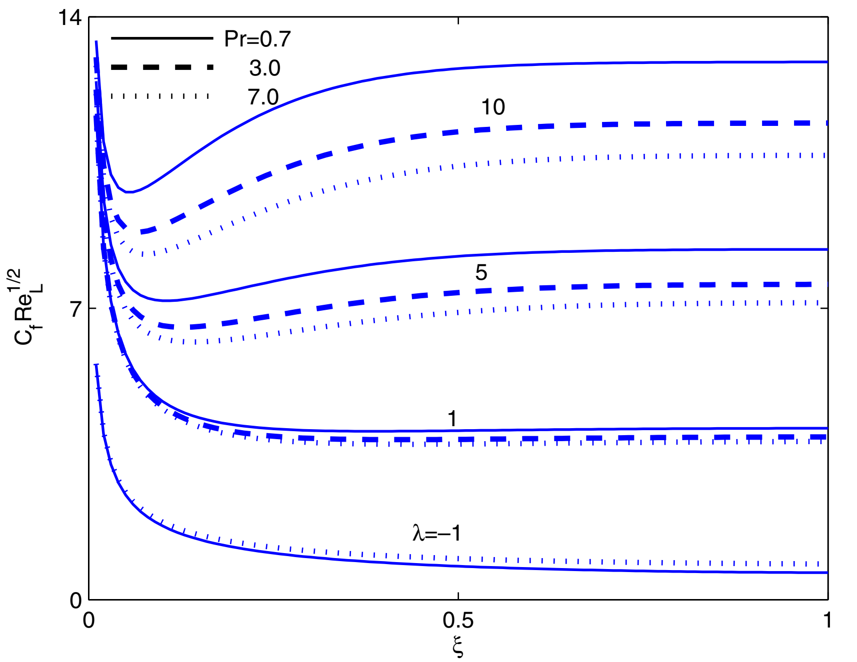

Fig. 6. Effects of Pr and λ on the skin friction coefficient ($C_f Re_L^{1/2}$) when $Sc = 0.22$ and $N = 0.5$.

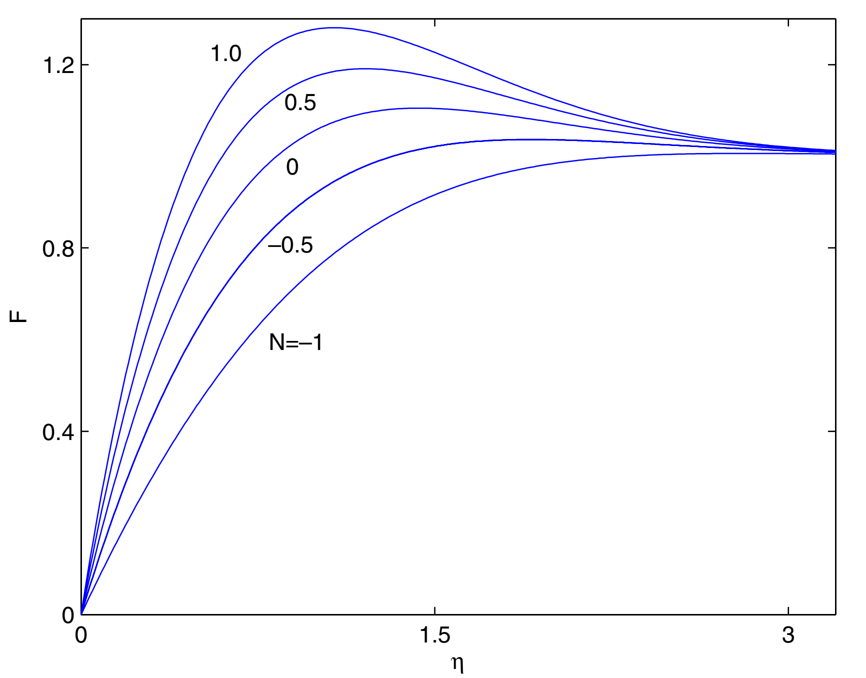

Fig. 7. Effect of N on the velocity profile when $Pr = 0.7$, $Sc = 0.94$ and $\lambda = 5$ at $\xi = 0.5$.

Also, the effects of λ and Prandtl number Pr on the skin friction coefficient $(C_f Re_L^{1/2})$ is shown in Fig. 6, it shows the oscillating trend in the skin friction coefficient for higher λ near the stagnation region and reach the steady state as $\xi(t^* \to \infty) = 1$. Physically these oscillations are due to the surplus convection of momentum within the boundary layer.

Figs. 7 and 8 show the effect of various N (ratio of concentration buoyancy force to thermal buoyancy force parameters) on the velocity profiles and surface shear stress parameters $(F, F_\eta(\xi, 0))$. The results presented in Fig. 7 indicate that for a fixed $\lambda = 5$, the velocity overshoot is observed for positive values of N and the magnitude of the overshoot increases further with the increase of N.

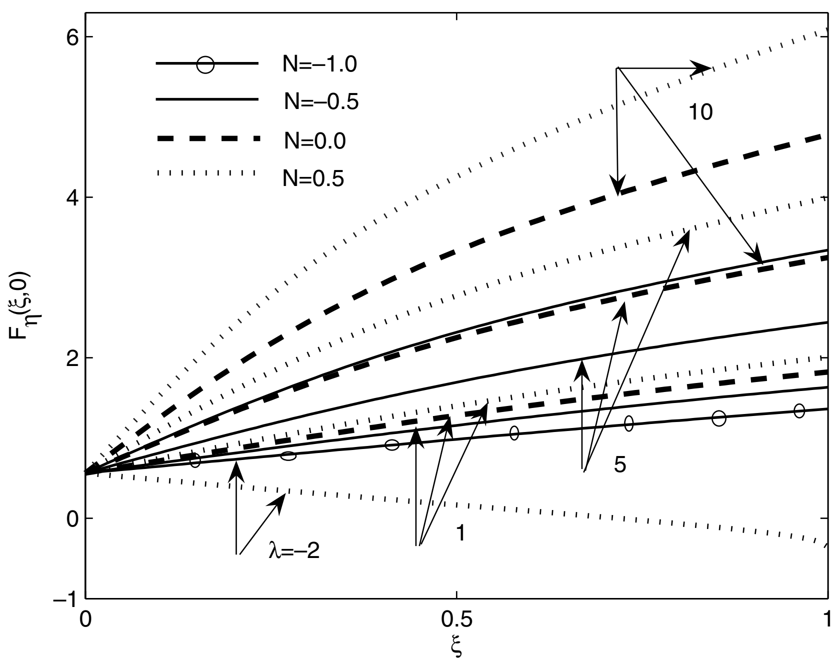

Fig. 8. Effects of N and λ on the surface shear stress parameters $F_\eta(\xi, 0)$ when $Pr = 0.7$ and $Sc = 0.94$.

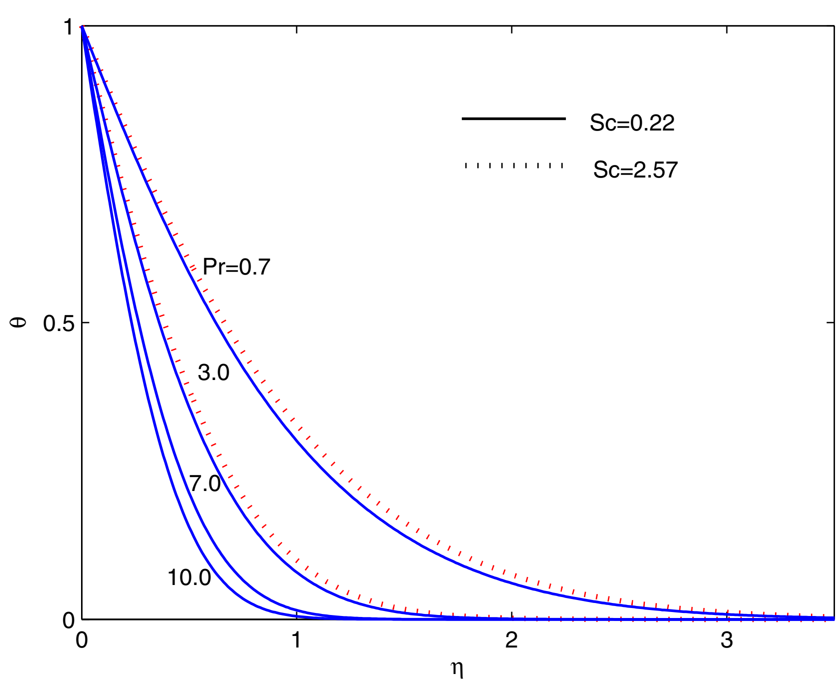

Fig. 9. Effects of Pr and Sc on the temperature profile when $\lambda = 10$ and $N = 0.5$ at $\xi = 0.5$.

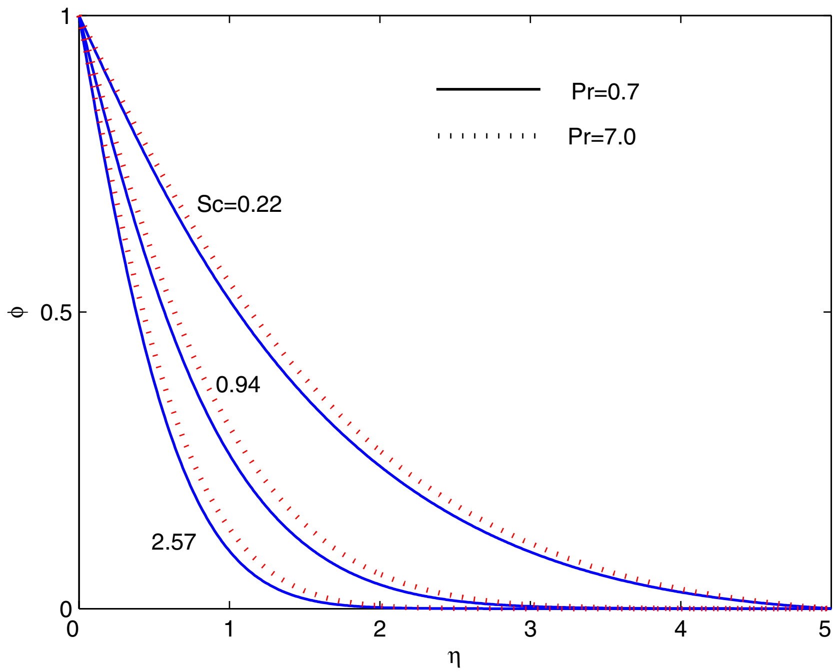

Fig. 10. Effects of Pr and Sc on the concentration profile when $\lambda = 10$ and $N = 0.5$ at $\xi = 0.5$.

The physical reason is that the assisting buoyancy force acts like a favorable pressure gradient which accelerate the fluid for low Prandtl number (air, $Pr = 0.7$) causing the velocity overshoot within the boundary layer. Due to the increase in the values of λ and N, the surface shear stress parameter ($F_\eta(\xi, 0)$) increases at every ξ locations and also for the fixed values of the λ and N, surface shear stress ($F_\eta(\xi, 0)$) increases with ξ which can be seen in Fig. 8. At $\xi = 0$ momentum equation is independent of the λ and N so the results are same for all λ and N which can be seen in Fig. 8 that all the lines are converging to a point at $\xi = 0$. The effects of λ and N on the temperature and concentration profiles are very small because the physical parameter λ and N appear only in the momentum equation. Hence, the effects of λ and N on those quantities are not displayed here.

Figs. 9 and 10 display the effects of Prandtl number (Pr) and Schmidt numbers (Sc) on the temperature and concentration profiles (θ, ϕ) for $\lambda = 10$ and $N = 0.5$ at $\xi = 0.5$. It is noticed that the increase in Pr and Sc number causes a reduction in the thermal boundary layer thickness and concentration boundary layer thickness, respectively. Consequently, the heat transfer at wall increases with Pr and the concentration gradient at wall increases with Sc. It may be noted that for steady state case i.e. at $\xi = 1$, similar observation have been made by Khair and Bejan [16] for a particular case of two-dimensional natural convection flow. Further, it may be noted that the effect of Pr on concentration gradient at wall and the effect of Sc on heat transfer rate at wall are comparatively small as can be seen in Figs. 9 and 10. The reason for this trend is that the temperature equation is independent to the Sc number and concentration equation is independent to the Prandtl number Pr.

6. Conclusions

Unsteady mixed convection flow over a vertical cone due to impulsive motion under the combined effects of thermal and mass diffusion has been studied numerically to obtain semi-similar solutions. It is observed that the buoyancy force produces significant velocity overshoot near the wall within the boundary layer for low Prandtl number fluid (air, $Pr = 0.7$) but for high Prandtl number fluid (water, $Pr = 7.0$) the velocity overshot is not much significant. The magnitude of the overshoot increases with the buoyancy parameter λ and the positive ratio of buoyancy parameter N. Further, the surface shear stress, surface heat transfer rate and concentration gradient at wall increase with the increase of λ. The numerical results illustrate that the surface heat transfer rate can be reduced by using low Prandtl number fluid. It is found that there is a smooth transition from the initial state to the final steady state and the steady state results (as $t \to \infty$) are corresponding to the results $\xi = 1$.

References

[1] S. Roy, D. Anilkumar, Unsteady mixed convection from a rotating cone in a rotating fluid due to the combined effect of thermal and mass diffusion, Int. J. Heat Mass Transfer 47 (2004) 1673–1684.
[2] R.G. Hering, R.J. Grosh, Laminar free convection from a non-isothermal cone, Int. J. Heat Mass Transfer 5 (1962) 1059–1068.
[3] R.G. Hering, Laminar free convection from a non-isothermal cone at low Prandtl numbers, Int. J. Heat Mass Transfer 8 (1965) 1333–1337.
[4] E.M. Sparrow, L.D.F. Guinle, Devitations from classical free convection boundary layer theory at low Prandtl number, Int. J. Heat Mass Transfer 11 (1968) 1403–1406.

[5] S. Roy, Free convection from a vertical cone at high Prandtl number, J. Heat Transfer 96 (1974) 115–117.
[6] H. Hasan, A.S. Majumdar, Double diffusive mixed convection flow along a vertical cone under the combined buoyancy effect of thermal and species diffusion, Int. J. Energy Res. 9 (1985) 129.
[7] M. Kumari, I. Pop, G. Nath, Mixed convection along a vertical cone, Int. Commun. Heat Mass Transfer 16 (1984) 99–106.
[8] M.C. Ece, An initial boundary layer flow past a translating and spinning rotational symmetric body, J. Eng. Math. 26 (1992) 415–428.
[9] M. Kumari, Development of flow and heat transfer on a wedge with a magnetic field, Arch. Mech. 49 (1977) 977–990.
[10] Rajeshwari Seshadri, Nalini Sreeshylan, G. Nath, Unsteady mixed convection flow in the stagnation region of a heated vertical plate due to impulsive motion, Int. J. Heat Mass Transfer 45 (2002) 1345–1352.
[11] J.C. William, T.B. Rhyne, Boundary layer development on a wedge impulsively set into motion, SIAM J. Appl. Math. 38 (1980) 215–224.
[12] H. Schlichting, Boundary Layer Theory, Springer, 2000, pp. 86–89.
[13] K. Inoyue, A. Tate, Finite differences version of quasilinearization applied to boundary layer equations, AIAA J. 12 (1974) 558–560.
[14] S. Roy, P. Saikrishnan, Non-uniform slot injection (suction) into steady laminar boundary layer flow over a rotating sphere, Int. J. Heat Mass Transfer 46 (2003) 3389–3396.
[15] R.S. Varga, Matrix Iteration Analysis, Prentice Hall, 2000.
[16] K.R. Khair, A. Bejan, Mass transfer to natural convection boundary layer flow driven by heat transfer, J. Heat Transfer 107 (1985) 979–981.